View metadata, citation and similar papers at core.ac.uk

brought to you by CORE

provided by NASA Technical Reports Server

NASA TECHNICAL NOTE

NASA TN D-5884

C.1

LOAN COPY: RETUR
AFWL (WLOL)
KIRTLAND AFB, N

0132647

TECH LIBRARY KAFB, NM

NASA TN D-5884

ANALYSIS OF SUPERSONIC CONICAL FLOWS

by C. W. Chiang and Richard D. Wagner, Jr.

Langley Research Center
Hampton, Va. 23365

NATIONAL AERONAUTICS AND SPACE ADMINISTRATION • WASHINGTON, D. C. • JULY 1970

TECH LIBRARY KAFB, NM
0132647

1. Report No.	2. Government Accession No.	3. Recipient's Catalog No.
NASA TN D-5884		

4. Title and Subtitle	5. Report Date
ANALYSIS OF SUPERSONIC CONICAL FLOWS	July 1970
	6. Performing Organization Code

7. Author(s)	8. Performing Organization Report No.
C. W. Chiang and Richard D. Wagner, Jr.	L-7082
	10. Work Unit No.
9. Performing Organization Name and Address	126-13-10-23
NASA Langley Research Center Hampton, Va. 23365	11. Contract or Grant No.
	13. Type of Report and Period Covered
12. Sponsoring Agency Name and Address	Technical Note
National Aeronautics and Space Administration Washington, D.C. 20546	14. Sponsoring Agency Code

15. Supplementary Notes

16. Abstract

An analytical technique is described for conical flow-field predictions for a particular class of flows. That is, problems of accelerating and decelerating supersonic cross flows are considered; the accelerating cross flow is produced when the free stream is normal to the conical axis of symmetry (a fin or stabilizer), and the decelerating cross flow is produced when the free stream is in the plane of symmetry (delta wing). For the first problem the solution is complete; for the latter only the solution for the supersonic cross-flow region is presented.

The fundamental differential equations are transformed into a dimensionless conical coordinate system. Since the partial differential equations governing a conical flow field are of hyperbolic type in regions of supersonic cross flow, the method of characteristics can be applied. The characteristic equations and compatibility equations are derived. Numerical computations are performed, starting from the leading edge and proceeding to the central portion of the wing.

17. Key Words (Suggested by Author(s))	18. Distribution Statement
Supersonic conical flow Delta wing Accelerating and decelerating cross flow Method of characteristics	Unclassified – Unlimited

19. Security Classif. (of this report)	20. Security Classif. (of this page)	21. No. of Pages	22. Price*
Unclassified	Unclassified	34	$3.00

*For sale by the Clearinghouse for Federal Scientific and Technical Information
Springfield, Virginia 22151

ANALYSIS OF SUPERSONIC CONICAL FLOWS

By C. W. Chiang* and Richard D. Wagner, Jr.
Langley Research Center

SUMMARY

An analytical technique is described for conical flow-field predictions for a particular class of flows. That is, problems of accelerating and decelerating supersonic cross flows are considered; the accelerating cross flow is produced when the free stream is normal to the conical axis of symmetry (a fin or stabilizer), and the decelerating cross flow is produced when the free stream is in the plane of symmetry (delta wing). For the first problem the solution is complete; for the latter only the solution for the supersonic cross-flow region is presented.

The fundamental differential equations are transformed into a dimensionless conical coordinate system. Since the partial differential equations governing a conical flow field are of hyperbolic type in regions of supersonic cross flow, the method of characteristics can be applied. The characteristic equations and compatibility equations are derived. Numerical computations are performed, starting from the leading edge and proceeding to the central portion of the wing.

INTRODUCTION

Linearized theory has been widely used to predict aerodynamic data for slender bodies at small angles of attack. For high Mach numbers, especially in the hypersonic range, nonlinear effects become important and the results obtained by the use of linearized theory are of little value. In fact, at high Mach numbers even the second-order theory is not adequate, and meaningful results can be obtained only from analyses including nonlinear effects. The present work is one phase of a program initiated to develop analytical techniques for flow-field predictions of a particular class of flows, taking into account nonlinear effects. Only conical flows will be considered.

Conical flow can be obtained over a conical body; that is, a body whose surface is generated by straight lines through a common apex. In conical flow, the flow properties along any ray directed from the vertex remain uniform, a feature which allows a transformation from a three-dimensional Cartesian coordinate system into a two-dimensional

*NRC-NASA Resident Research Associate, on leave from the University of Denver.

conical coordinate system. Thus computations are greatly simplified. Many component parts of supersonic vehicles are conical; a flat delta wing is a typical example.

Numerous examples of the application of linearized theory to supersonic conical flows exist in the literature (refs. 1 to 3). The system of rotational conical-flow equations has been considered by several investigators (refs. 4 to 15). These analyses show that the character of the transformed equations is determined by the cross-flow Mach number (i.e., the component of the local Mach number normal to the ray from the apex). If the cross flow is subsonic, sonic, or supersonic, the equations are elliptic, parabolic, or hyperbolic, respectively. In the present paper, only flows for which the cross flow is supersonic are considered. This restriction allows the use of the method of characteristics for numerical computations.

Problems of accelerating and decelerating supersonic cross flows are considered. As shown in figure 1, an accelerating cross flow is produced when the free stream is normal to the conical axis of symmetry (a fin or stabilizer), while a decelerating cross flow is produced when the free stream is parallel to the plane of symmetry of the wing as occurs with a delta wing. For the latter problem, solutions for the supersonic cross-flow region prevail until the cross flow approaches sonic (though in many cases nearly the entire wing is covered); for accelerating cross flows, a complete solution is obtained for a symmetrical body.

SYMBOLS

a dimensionless sonic velocity (actual sonic velocity divided by V_∞)

a_1,a_2,a_3 defined by equations (17)

b_1,b_2,b_3,b_4 defined by equations (19)

C_p surface pressure coefficient

c_v specific heat at constant volume

h enthalpy

M Mach number

$\hat{n}$ unit normal to the surface

p pressure

S entropy; also shock point

s dimensionless entropy, $\frac{S - S_0}{\gamma(\gamma - 1)c_v}$

T temperature

$U = \frac{V}{V_\infty}$

u,v,w dimensionless velocity components along X-, Y-, and Z-axis, respectively (actual velocity components divided by V_∞)

V velocity

X,Y,Z Cartesian coordinate axes (fig. 1)

x,y,z coordinates along X-, Y-, and Z-axis, respectively

α angle of attack

$\alpha_1 = \tan^{-1}\left(\frac{\tan \alpha}{\cos \chi}\right)$

$\beta = \cos^{-1}(\sin \chi \cos \alpha)$

Γ complement of angle between the surface normal and the stream direction

γ ratio of specific heats

Δ incremental

∇ gradient vector operator

δ flow deflection angle

$\epsilon = \phi_1 + \alpha_1$

$\zeta = \frac{\xi u - w}{\eta u - v}$

$\eta = \frac{y}{x}$

θ defined in figure 3

$\xi = \frac{z}{x}$

$\xi_{s,max}$ ξ-coordinate of upper surface of airfoil at geometrical plane of symmetry

ρ density

$\phi_1 = \tan^{-1}\left(\frac{\xi}{\cos \chi - \eta \sin \chi}\right)$

$\phi_2 = \tan^{-1}\left(\sin \chi \tan \phi_1\right)$

χ angle between Y-axis and leading edge of airfoil (see fig. B1)

ω dimensionless vorticity vector

$\times, \cdot$ cross multiply, dot multiply

Subscripts:

L leading-edge condition

N normal to the leading edge

n normal to the shock

o reference condition

s at the surface

t tangential

σ behind the shock

I first given condition

∞ free stream

+,-	characteristic directions
x,y,z,η,ξ	partial differentiation with respect to x, y, z, η, and ξ

Accent:

$\hat{}$	unit vector

FUNDAMENTAL EQUATIONS

A rectangular Cartesian coordinate system with origin at the vertex of a delta wing is shown in figure 1. The X-axis is directed from the origin along the axis of symmetry of the lower surface of the wing. The upper surface of the wing is fixed by the profile normal to the X-axis; lenticular and parabolic profiles are used in the numerical calculations to be presented. Only attached leading-edge shocks are considered herein, and hence the upper and lower wing surfaces are independent.

Flow Equations

For steady flow of an ideal gas with a uniform free stream, the continuity, momentum, and energy equations may be written in the form (ref. 16)

$$\nabla \cdot (\rho U) = 0 \tag{1}$$

$$\omega \times U = \frac{T}{V_\infty{}^2} \nabla S \tag{2}$$

$$U \cdot \nabla S = 0 \tag{3}$$

where U is a dimensionless velocity vector, actual velocity divided by free-stream velocity V_∞.

Flow Equations in Cartesian Coordinates

The momentum and energy equations (2) and (3) may be written in Cartesian coordinates in the form

$$w\left(u_z - w_x\right) - v\left(v_x - u_y\right) = a^2 s_x \tag{4a}$$

$$u\left(v_x - u_y\right) - w\left(w_y - v_z\right) = a^2 s_y \tag{4b}$$

$$v\left(w_y - v_z\right) - u\left(u_z - w_x\right) = a^2 s_z \tag{4c}$$

$$us_x + vs_y + ws_z = 0 \tag{4d}$$

where

u,v,w dimensionless velocity components along X-, Y-, and Z-axis, actual velocity components divided by V_∞

s dimensionless entropy, $\dfrac{S - S_0}{\gamma(\gamma - 1)c_v} = \dfrac{1}{\gamma(\gamma - 1)} \ln \dfrac{p/p_\infty}{\rho^\gamma/\rho_\infty{}^\gamma}$

S_0 reference entropy

a dimensionless sonic velocity, actual sonic velocity divided by V_∞

Flow Equations in Conical Coordinates

In dimensionless conical coordinates the position of a straight line directed from the apex of the conical body is determined by the coordinates $\eta = y/x$ and $\xi = z/x$. The partial-derivative operators in the X,Y,Z axis system may be written in conical coordinates as follows:

$$\left.\begin{aligned} \frac{\partial}{\partial x} &= -\frac{1}{x}\left(\eta \frac{\partial}{\partial \eta} + \xi \frac{\partial}{\partial \xi}\right) \\ \frac{\partial}{\partial y} &= \frac{1}{x} \frac{\partial}{\partial \eta} \\ \frac{\partial}{\partial z} &= \frac{1}{x} \frac{\partial}{\partial \xi} \end{aligned}\right\} \tag{5}$$

By using the partial-derivative operators of equations (5), equations (4) may be written in conical coordinates (ref. 4):

$$v\left(\eta v_\eta + \xi v_\xi + u_\eta\right) + w\left(\eta w_\eta + \xi w_\xi + u_\xi\right) = -a^2\left(\eta s_\eta + \xi s_\xi\right) \tag{6a}$$

$$u\left(\eta v_\eta + \xi v_\xi + u_\eta\right) + w\left(w_\eta - v_\xi\right) = -a^2 s_\eta \tag{6b}$$

$$u\left(\eta w_\eta + \xi w_\xi + u_\xi\right) + v\left(v_\xi - w_\eta\right) = -a^2 s_\xi \tag{6c}$$

$$(\eta u - v)s_\eta + (\xi u - w)s_\xi = 0 \tag{6d}$$

Only the last three of equations (6) are independent, and equation (6a) is not used. As shown in appendix A, the continuity equation (1) may be written in conical coordinates in the form

$$2a^2\left(\eta u_\eta + \xi u_\xi - v_\eta - w_\xi\right) - (\eta u - v)U_\eta{}^2 - (\xi u - w)U_\xi{}^2 = 0 \tag{7}$$

Boundary Conditions

The boundary conditions are given at the body surface and at the shock (details are shown in appendix B). The boundary condition at the body is that the normal velocity components vanish. Therefore,

$$\left(\frac{d\xi}{d\eta}\right)_s = \frac{\xi u - w}{\eta u - v} \tag{8}$$

The boundary conditions at the shock can be found by applying the Rankine-Hugoniot relations across the shock. To facilitate the application of the shock conditions, a fictitious plane shock which is tangent to the body shock is introduced. The flow properties across this shock will match those behind the body shock at the point of tangency. In a plane which is normal to the fictitious leading edge, and hence the fictitious shock plane, the angle ϵ between the fictitious shock plane and the plane of the undisturbed flow may be determined for known values of the free-stream Mach number M_∞, the angle of attack α, the flow deflection angle δ, and the sweep angle χ, from the following equation:

$$\left(1 + \frac{\gamma - 1}{2} M_\infty{}^2 \sin^2\beta\right)\tan^3\epsilon - \left(M_\infty{}^2 \sin^2\beta - 1\right)\cot\left(\alpha_1 + \delta\right)\tan^2\epsilon$$
$$+ \left(1 + \frac{\gamma + 1}{2} M_\infty{}^2 \sin^2\beta\right)\tan\epsilon + \cot\left(\alpha_1 + \delta\right) = 0 \tag{9}$$

Once the angle ϵ is determined, the velocity components behind the shock and the entropy change across the shock can be found.

The velocity components behind the shock for the problem of decelerated cross flow (wing problem) are

$$\left.\begin{aligned} u &= \cos\beta \sin\chi + \frac{\cos\chi \cos\delta \sin\beta \cos\epsilon}{\cos\left(\epsilon - \alpha_1 - \delta\right)} \\ v &= -\cos\beta \cos\chi + \frac{\sin\chi \cos\delta \sin\beta \cos\epsilon}{\cos\left(\epsilon - \alpha_1 - \delta\right)} \\ w &= \frac{\sin\delta \sin\beta \cos\epsilon}{\cos\left(\epsilon - \alpha_1 - \delta\right)} \end{aligned}\right\} \tag{10}$$

Similarly, for the problem of accelerated cross flow (fin problem), the velocity components behind the shock are in the form

$$\left.\begin{aligned} u &= -\cos\beta \sin\chi + \frac{\cos\chi \cos\delta \sin\beta \cos\epsilon}{\cos(\epsilon - \alpha_1 - \delta)} \\ v &= \cos\beta \cos\chi + \frac{\sin\chi \cos\delta \sin\beta \cos\epsilon}{\cos(\epsilon - \alpha_1 - \delta)} \\ w &= \frac{\sin\delta \sin\beta \cos\epsilon}{\cos(\epsilon - \alpha_1 - \delta)} \end{aligned}\right\} \tag{11}$$

The entropy change across the shock is calculated from

$$\nabla s = s - s_\infty$$

$$= \frac{1}{\gamma(\gamma - 1)} \ln\left[\frac{2\gamma}{\gamma + 1}\left(M_\infty{}^2 \sin^2\beta \sin^2\epsilon - \frac{\gamma - 1}{\gamma + 1}\right)\right] - \frac{1}{\gamma - 1} \ln\left[\frac{(\gamma + 1)M_\infty{}^2 \sin^2\beta \sin^2\epsilon}{2 + (\gamma - 1)M_\infty{}^2 \sin^2\beta \sin^2\epsilon}\right] \tag{12}$$

CHARACTERISTIC AND COMPATIBILITY EQUATIONS

Characteristic and compatibility equations are derived in detail in appendix C. In addition to boundary conditions, they constitute the necessary requirements for actual computations.

Along a stream surface a characteristic is given by

$$\frac{d\xi}{d\eta} = \frac{\xi u - w}{\eta u - v} \tag{13}$$

For this characteristic there is one compatibility relation due to constancy of entropy along stream surfaces:

$$ds = 0 \tag{14}$$

The second compatibility equation along stream surfaces may be written in the form

$$du + \eta\, dv + \xi\, dw = 0 \tag{15}$$

The remaining two characteristics, one above and one below the stream surface, have slopes given by

$$\left(\frac{d\xi}{d\eta}\right)_\pm = \frac{a_1 \pm \sqrt{a_1{}^2 - a_2 a_3}}{a_2} \tag{16}$$

where

$$\left.\begin{aligned} a_1 &= a^2\xi\eta - (\eta u - v)(\xi u - w) \\ a_2 &= a^2\left(1 + \eta^2\right) - (\eta u - v)^2 \\ a_3 &= a^2\left(1 + \xi^2\right) - (\xi u - w)^2 \end{aligned}\right\} \tag{17}$$

The compatibility equation corresponding to the two characteristics is

$$b_1\,du + b_2\,dv + b_3\,dw + b_4\,ds = 0 \tag{18}$$

where

$$\left.\begin{aligned} b_1 &= -a^2\left(\xi v - \eta w\right) - \left(a_1 - a_2\frac{d\xi}{d\eta}\right)u \\ b_2 &= a_2\left[(\xi u - w) - (\eta u - v)\frac{d\xi}{d\eta}\right] - a^2\eta(\xi v - \eta w) - \eta u\left(a_1 - a_2\frac{d\xi}{d\eta}\right) \\ b_3 &= -a^2\xi(\xi v - \eta w) - \xi u\left(a_1 - a_2\frac{d\xi}{d\eta}\right) + \frac{a_3 a_2\left[(\xi u - w) - (\eta u - v)\frac{d\xi}{d\eta}\right]}{a_2\frac{d\xi}{d\eta}} \\ b_4 &= -a^2\left(a_1 - a_2\frac{d\xi}{d\eta}\right) \end{aligned}\right\} \tag{19}$$

METHOD OF COMPUTATION

The application of the method of characteristics to compute conical flow fields consists of the repeated use of three basic computing processes (one each for the shock point, the body point, and the general field point) proceeding inward from the leading edge with given initial conditions. With reference to figure 2, the initial conditions are established by approximating the leading portion of the wing by a swept wedge, tangent to the wing at η_I. The oblique-shock solution, equations (12) and (10) or (11), then gives the flow conditions at the initial station η_I.

Shock Point

To determine the ξ-coordinate of the shock at $\eta = \eta_I + \Delta\eta$, as a first approximation the shock at η_I is extended to $\eta_I + \Delta\eta$ to establish the point S. The shock relations give the first approximation to the flow properties at S, and the characteristic SA_1 establishes the point A_1. The flow at point A_1 is known by interpolation, and the compatibility relation, equation (18), must be satisfied for the characteristic SA_1 as well as

the shock conditions at S. An iteration on the shock angle at S, with averaged coefficients in the compatibility equations, allows determination of the correct shock angle and the correct locations of S and A_1, and thence the flow properties at point S.

Body Point

The point A_p on the characteristic A_pP_p intersecting the body at $\eta = \eta_I + \Delta\eta$ can be found by interpolation. The compatibility relation for A_pP_p, the two compatibility relations for the streamline characteristics (eqs. (14) and (15)), and the boundary condition (eq. (8)) can then be solved for the flow conditions at P_p.

General Field Point

The present calculations were performed by computing conditions from the shock to the body. After the point A_1 is established, the characteristic A_1P_1 locates the first field point P_1. The streamline P_1B_1 and the characteristic C_1P_1 through P_1 can be determined by interpolation of the given, or known, conditions on η_I. The compatibility equations for the characteristics A_1P_1 and C_1P_1 and the two compatibility equations for the streamline P_1B_1 can then be solved for the flow conditions at point P_1. This process is repeated for the point P_2, and so on, until a point P_f is reached with the characteristic P_fC_f intersecting the initial data line $\eta = \eta_I$ (or the current known data line) below the body surface. The body point is then calculated; the flow conditions are then completely specified along the line $\eta = \eta_I + \Delta\eta$, from the shock to the body. This new set of data can be used to establish the conditions at the next station, $\eta = \eta_I + 2\Delta\eta$. The computations thus proceed over the wing, or fin, until the sonic condition is obtained, or the trailing edge is reached.

The method as presented with iterations and quadratic interpolations for the flow properties is accurate to second order (i.e., the truncation error is the order of the mesh size cubed). This computational method was programed in FORTRAN language for computing on an electronic digital computer.

APPLICATIONS

Accelerating Cross Flows (Fin Problems)

Calculated pressure distributions for fins with circular-arc profiles are shown in figure 3. The results are given in terms of the ratio of the local surface pressure coefficient C_p to the maximum pressure coefficient $C_{p,L}$, which occurs at the leading edge. The fin geometry is defined by the sweep angle χ and the initial flow deflection δ_N in a plane normal to the leading edge. Calculations for $M_\infty = 6$, 10, and 30 were performed for fins with $\chi = 30^o$ and $\delta_N = 5^o$ and 20^o. The results are presented up to the geometrical plane of symmetry of the fin, $\theta = 180^o$ (θ is defined in fig. 3), although actual calculations were carried beyond that. Calculations can be carried close to the trailing edge

with much finer meshes and longer computing time. Included in figure 3 are calculations based on a shock-expansion method for conical flows which was obtained in reference 17. The agreement of the two methods is exceptional, considering the simplicity of the shock-expansion approach. Because earlier studies have shown that the two-dimensional shock-expansion method works best at high values of γ, a cursory examination of the effect of γ was made. In figure 4 calculations are shown for a fin with a circular-arc profile, $\alpha = 0^{\circ}$, $\delta_N = 30^{\circ}$, $\chi = 60^{\circ}$, and $M_\infty = 30$ at $\gamma = 1.667$, 1.400, and 1.100. The shock-expansion method works best for $\gamma = 1.400$ and the poorest agreement is for $\gamma = 1.100$. These results are consistent with the γ-effect observed in the prediction of two-dimensional flows by two-dimensional shock expansion.

For two-dimensional and axisymmetric flows, the application of the shock-expansion method is greatly simplified because of a closed-form relation between the surface pressure and the local surface inclination. For conical flows such a relation is not known and solutions can be obtained only by quadrature; more easily obtained approximate solutions are desirable. Newtonian theory is often used by the practicing engineer in the analysis of complex three-dimensional configurations. There are too few exact solutions to enable an assessment of the applicability of Newtonian theory to three-dimensional hypersonic flows. Indeed, there has been no assurance that the usefulness of Newtonian theory for two-dimensional and axisymmetric flows should prevail for three-dimensional flows. In figure 5, results obtained from Newtonian theory have been included for comparison with results obtained by the method of characteristics, the shock-expansion method, and a strip theory. The last of these is a two-dimensional approximation using the circular profile and two-dimensional shock-expansion theory. The Newtonian theory used is a logical extension of the generalized Newtonian theory (ref. 18) and the pressure ratio is given by

$$\frac{C_p}{C_{p,L}} = \frac{\sin^2 \Gamma}{\sin^2 \Gamma_L}$$

where Γ is the complement of the angle between the surface normal and the stream direction, and $C_{p,L}$ is the pressure coefficient at the leading edge, where $\Gamma = \Gamma_L$, obtained from the oblique-shock relations for the tangent swept wedge. The ratio of the surface pressure to leading-edge surface pressure was calculated at $\gamma = 1.667$ and 1.400 for a fin with $\delta_N = 20^{\circ}$, $\chi = 30^{\circ}$, and $M_\infty = 30$. Strip theory always underestimates the pressure and the Newtonian theory gives poor results in the low-pressure regions (a general failing of Newtonian theory; see ref. 19).

In figure 6 are shown comparisons at $M_\infty = 6.85$ between the method of characteristics, shock-expansion method, and unpublished experimental data obtained by M. H. Bertram at the NASA Langley Research Center. In these tests the ratio of wall temperature to total temperature was in the range of 0.6 to 0.8, the free-stream Reynolds number

was 0.31×10^6 per inch (0.12×10^6 per cm), the root-chord length was 4.8 inches (12.2 cm), and the semispan was 2.4 inches (6.1 cm). The local chord was 2.38 inches (6.05 cm) at the section in which the pressure orifices were located. The profile of the surface consists of two parabolas in the YZ-plane, tangent at $\eta = \sqrt{3}/2$; namely,

$$\xi = q \tan \chi(\eta \cot \chi - 0.5)^2$$

where $q = 0.1$ for $\sqrt{3}/2 < \eta \leqq \sqrt{3}$ and $q = 0.05$ for $0 \leqq \eta < \sqrt{3}/2$. The maximum thickness occurs at $\eta = \sqrt{3}/2$. In figure 6, $\chi = 30^\circ$, and $\delta_N \approx 11^\circ$ at $\alpha = 0^\circ$. The two theoretical solutions agree well, and the difference between the experimental data and theory can be attributed to the viscous boundary-layer displacement effects (ref. 20). At $\alpha = 10^\circ$ the theory and experimental results are quite close.

Decelerating Cross Flows (Wing Problems)

In the case of a delta wing where the free-stream velocity vector lies in the plane of symmetry, the cross flow is supersonic at the leading edge and decelerates to subsonic and ultimately to zero at the plane of symmetry. The present calculations can be used only in the region of supersonic cross flow, but this flow region can constitute a major portion of the flow field. (For example, for a circular-arc wing with $M_\infty = 30$, $\delta_N = 20^\circ$, and $\chi = 30^\circ$, about 90 percent of the wing flow field can be computed.)

Calculations for a circular-arc wing are shown in figure 7. The wing parameters are $\delta_N = 9^\circ 18'$ and $\chi = 50^\circ$. The shock shape and the pressure ratio of both the shock and the wing surface are given for $M_\infty = 4.0$ and $\alpha = 0^\circ$, 5°, and 10°. For this case the method of characteristics can be used to compute a major portion of the flow field, until the cross flow approaches sonic as shown in figure 7(a). As the angle of attack increases, the portion of supersonic cross flow decreases. A line of constant cross-flow Mach number of 1.08 for the case of $\alpha = 0^\circ$ is also shown in figure 7(a) to give some idea of the Mach cone which separates the supersonic and subsonic cross flows. In reference 21 calculations based on the method of lines, giving a solution for the entire flow field, are presented for the same conditions; these are shown in figure 7(b). The agreement of the two methods is excellent. The pressure ratio calculated on the basis of Newtonian theory is also shown; it has lower values in the supersonic region than the other two methods.

An additional comparison of the method of reference 21 with the method of characteristics is given in figure 8, which shows the surface pressure coefficient on a circular-arc wing with $\chi = 50^\circ$, $\delta_N = 20^\circ$, $\alpha = 10^\circ$, and $M_\infty = 8.1$. Also included in figure 8 is the shock-expansion method. All the methods show excellent agreement. The shock shapes predicted by the method of characteristics and the method of lines also are

compared and they agree closely. In reference 21, the solutions by the present method and the method of lines are compared and verified with experimental data.

CONCLUDING REMARKS

An analytical technique using the method of characteristics has been described for flow predictions of accelerated and decelerated supersonic cross flows over a conical body. Results obtained by this method agree well with experimental results and other analytical results.

Langley Research Center,
National Aeronautics and Space Administration,
Hampton, Va., April 28, 1970.

APPENDIX A

CONTINUITY EQUATION IN CONICAL COORDINATES

The entropy function can be written in the form

$$\frac{p}{\rho^{\gamma}} = \frac{p_{\infty}}{\rho_{\infty}{}^{\gamma}} e^{\gamma(\gamma-1)s} = f(s) \tag{A1}$$

and enthalpy may be written in the form

$$h = \frac{\gamma}{\gamma - 1}\frac{p}{\rho V_{\infty}{}^2} = \frac{1}{\gamma - 1} a^2 \tag{A2}$$

Combining equations (A1) and (A2) gives

$$\rho = k_1\left(a^2\right)^{\frac{1}{\gamma-1}}\left[f(s)\right]^{-\frac{1}{\gamma-1}} \tag{A3}$$

where

$$k_1 = \left(\frac{V_{\infty}{}^2}{\gamma}\right)^{\frac{1}{\gamma-1}}$$

When equation (A3) is substituted into equation (1) in the body of the paper, the continuity equation becomes

$$\begin{aligned}\nabla \cdot (\rho U) &= k_1 \nabla \cdot \left[a^{\frac{2}{\gamma-1}} f(s)^{-\frac{1}{\gamma-1}} U\right] \\ &= k_1 f(s)^{-\frac{1}{\gamma-1}} \nabla \cdot \left[a^{\frac{2}{\gamma-1}} U\right] - \frac{k_1}{\gamma - 1} f(s)^{-\frac{\gamma}{\gamma-1}}\left[a^{\frac{2}{\gamma-1}} U\right] \cdot \nabla f(s) \\ &= 0\end{aligned}$$

Since $U \cdot \nabla S = 0$, then

$$U \cdot \nabla\left[f(s)\right] = \gamma(\gamma - 1) f(s) U \cdot \nabla s = 0$$

Thus

$$\nabla \cdot \left[a^{\frac{2}{\gamma-1}} U\right] = 0 \tag{A4}$$

but

$$a^2 = (\gamma - 1)\left(h_o - \frac{U^2}{2}\right) \tag{A5}$$

and combining equations (A4) and (A5) gives

$$2a^2 \nabla \cdot U - U \cdot \nabla U^2 = 0 \tag{A6}$$

Equation (A6), the continuity equation, may be written in conical coordinates as

$$2a^2\left(\eta u_\eta + \xi u_\xi - v_\eta - w_\xi\right) - (\eta u - v)U_\eta{}^2 - (\xi u - w)U_\xi{}^2 = 0 \tag{A7}$$

APPENDIX B

BOUNDARY CONDITIONS

The boundary condition at the body is that the normal velocity components vanish. If the equation at the conical surface is $g(\xi,\eta) = 0$, then the boundary condition at the body is

$$U \cdot \frac{\nabla g}{|\nabla g|} = 0$$

or

$$\left(\frac{d\xi}{d\eta}\right)_S = \frac{\xi u - w}{\eta u - v} \tag{B1}$$

The boundary conditions at the shock can be found by applying the Rankine-Hugoniot relations across the shock. The equations presented herein are extensions of those given in reference 4 for the conditions at the leading edge of a flat delta wing; they are generalized here to apply to any location along the shock contour. To help in understanding the relations in front of and behind the shock plane, a geometrical layout is constructed as shown in figures B1 and B2. To facilitate the application of the shock conditions, a

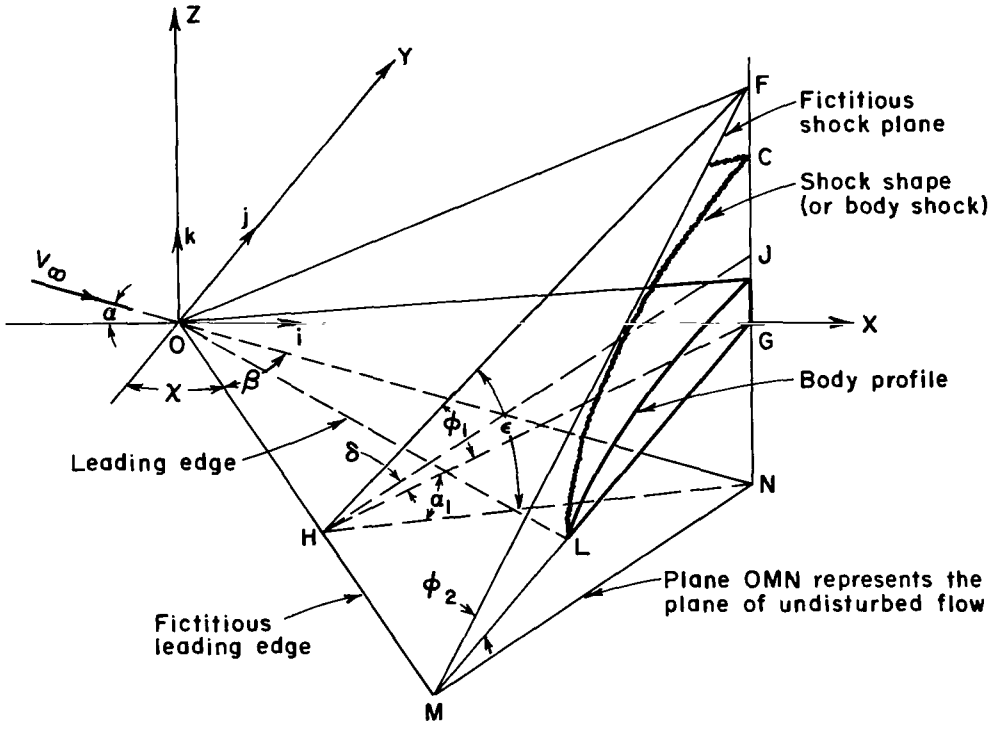

Figure B1.- Geometrical layout.

fictitious plane shock which is tangent to the body shock is introduced (plane OFM in fig. B1). The flow properties across this shock will match those across the body shock. The equation of the fictitious shock plane is (by geometry)

$$\tan \phi_1 = \frac{\xi}{\cos \chi - \eta \sin \chi} \tag{B2}$$

where ϕ_1 is the slope of the fictitious shock plane measured in the plane which is normal to the fictitious leading edge (in plane FHG).

The angle between the direction of the undisturbed flow and the fictitious leading edge, β, and the angles α_1 and ϕ_2 may be obtained through analysis of the geometry:

$$\beta = \cos^{-1}(\sin \chi \cos \alpha) \tag{B3}$$

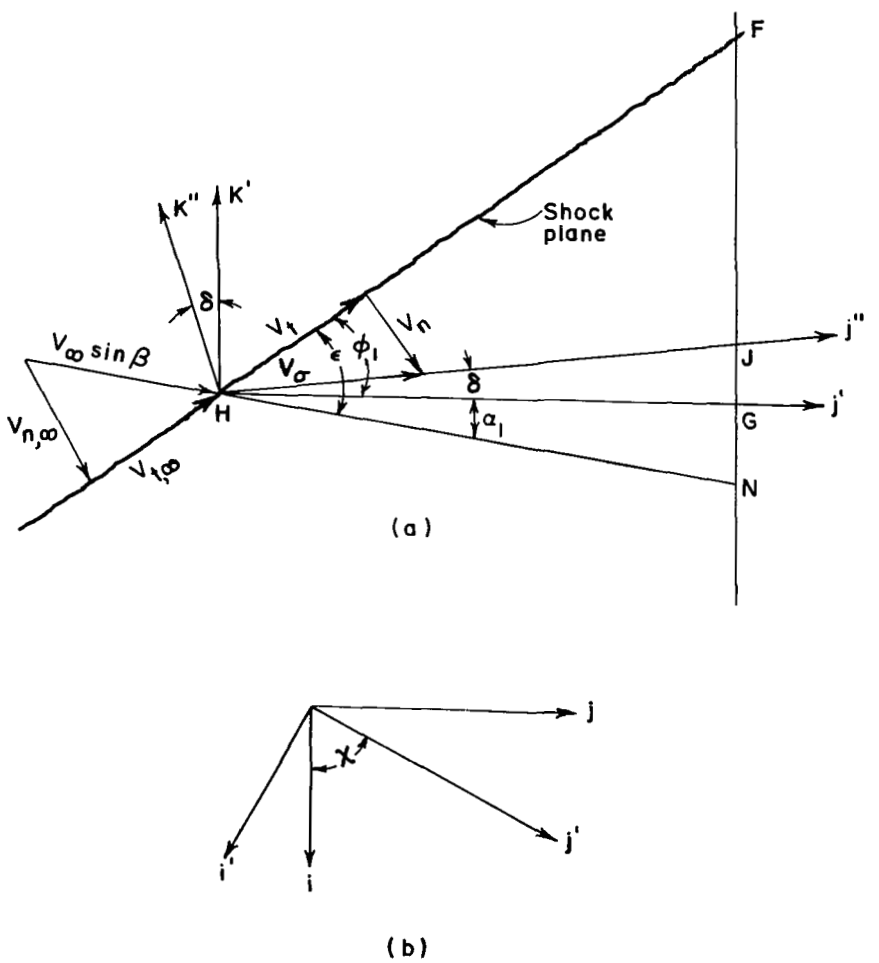

Figure B2.- Velocity components with rotating axes.

$$\alpha_1 = \tan^{-1}\left(\frac{\tan \alpha}{\cos \chi}\right) \tag{B4}$$

$$\tan \phi_2 = \sin \chi \tan \phi \tag{B5}$$

where ϕ_2 is the slope of the shock plane in the plane normal to the X-axis.

The plane FHN is redrawn in detail in figure B2(a). The free-stream velocity component in the direction of HN is $V_\infty \sin \beta$, and the normal and tangential free-stream velocity components are designated as $V_{n,\infty}$ and $V_{t,\infty}$, respectively. The resultant, normal, and tangential velocity components behind the shock are denoted by V_σ, V_n, and V_t, respectively.

At the leading edge of the fictitious-plane shock, the shock wave must satisfy the relation (ref. 22)

$$V_{n,\infty} \cdot V_n = (a^*)^2 - \frac{\gamma - 1}{\gamma + 1} V_t^2 \tag{B6}$$

where a^* is critical sonic velocity.

From figure B2 it is easily seen that

$$V_{t,\infty} = V_\infty \sin \beta \cos \epsilon \tag{B7}$$

$$V_{n,\infty} = V_\infty \sin \beta \sin \epsilon \tag{B8}$$

where $\epsilon = \phi_1 + \alpha_1$ represents the angle between the fictitious shock plane and the plane of undisturbed flow.

Since

$$V_t = V_{t,\infty}$$

$$V_n = V_{t,\infty} \tan\left(\epsilon - \delta - \alpha_1\right) = V_\infty \sin \beta \cos \epsilon \tan\left(\epsilon - \delta - \alpha_1\right) \tag{B9}$$

where δ is the angle between the cross-flow velocity and the XY-plane measured normal to the fictitious leading edge.

The energy equation may be written

$$h + \frac{V^2}{2} = h^* + \frac{(V^*)^2}{2}$$

or

$$a_\infty^2 + \frac{\gamma - 1}{2}\left(V_\infty \sin \beta\right)^2 = (a^*)^2 + \frac{\gamma - 1}{2}(a^*)^2 = \frac{\gamma + 1}{2}(a^*)^2$$

$$(a^*)^2 = \frac{2}{\gamma + 1} a_\infty^2 + \frac{\gamma - 1}{\gamma + 1}\left(V_\infty \sin \beta\right)^2 \tag{B10}$$

where V^* and a^* are critical velocity and critical sonic velocity.

Combining equations (B7), (B6), and (B10) yields

$$V_\infty^2 \sin^2\beta \sin \epsilon \cos \epsilon \tan\left(\epsilon - \delta - \alpha_1\right) = \frac{2}{\gamma + 1} a_\infty^2 + \frac{\gamma - 1}{\gamma + 1} V_\infty^2 \sin^2\beta - \frac{\gamma - 1}{\gamma + 1} V_\infty^2 \sin^2\beta \cos^2\epsilon$$

If $\tan\left(\epsilon - \delta - \alpha_1\right)$ is expanded, V_∞/a_∞ is replaced by M_∞, and both sides of the equation are divided by $\tan\left(\delta + \alpha_1\right)$, the result is

$$\left(1 + \frac{\gamma - 1}{2} M_\infty^2 \sin^2\beta\right)\tan^3\epsilon - \left(M_\infty^2 \sin^2\beta - 1\right)\cot\left(\delta + \alpha_1\right)\tan^2\epsilon$$
$$+ \left(1 + \frac{\gamma + 1}{2} M_\infty^2 \sin^2\beta\right)\tan \epsilon + \cot\left(\delta + \alpha_1\right) = 0 \tag{B11}$$

For known values of M_∞, α, δ, and χ, equation (B11) determines the angle ϵ; the velocity components behind the shock plane and the entropy change across the shock can then be calculated.

To obtain velocity components behind the shock, the reader is again referred to figure B2. The coordinate axes j',k' and j'',k'' are parallel and normal to HG and HJ, respectively. The coordinate axes i,j are parallel to the X-axis and Y-axis; the axis i' is in the direction of the fictitious leading edge, and the axis j' is normal to the axis i' and is in the direction of HG, which coincides with the XY-plane (see fig. B1).

By coordinate transformation, the unit vector in the direction of the velocity V_σ behind the shock is

$$\hat{j}'' = \hat{i} \cos \chi \cos \delta + \hat{j} \sin \chi \cos \delta + \hat{k} \sin \delta \tag{B12}$$

$$V_\sigma = \frac{V_\infty \sin \beta \cos \epsilon}{\cos\left(\epsilon - \delta - \alpha_1\right)} \tag{B13}$$

Equations (B12) and (B13) then define the magnitude and the direction of the velocity V_σ behind the shock. The total velocity is simply the vector sum of this velocity vector and the free-stream velocity component tangential to the leading edge, $V_\infty \cos \beta\left(\hat{i} \sin \chi - \hat{j} \cos \chi\right)$.

The velocity components behind the shock for the problem of decelerated cross flow (wing problem) are then

$$\left.\begin{aligned} u &= \cos\beta \sin\chi + \frac{\cos\chi \cos\delta \sin\beta \cos\epsilon}{\cos\left(\epsilon - \delta - \alpha_1\right)} \\ v &= -\cos\beta \cos\chi + \frac{\sin\chi \cos\delta \sin\beta \cos\epsilon}{\cos\left(\epsilon - \delta - \alpha_1\right)} \\ w &= \frac{\sin\delta \sin\beta \cos\epsilon}{\cos\left(\epsilon - \delta - \alpha_1\right)} \end{aligned}\right\} \tag{B14}$$

Similarly, for the problem of accelerated cross flow (fin problem), the velocity components behind the shock are

$$\left.\begin{aligned} u &= -\cos\beta \sin\chi + \frac{\cos\chi \cos\delta \sin\beta \cos\epsilon}{\cos\left(\epsilon - \delta - \alpha_1\right)} \\ v &= \cos\beta \cos\chi + \frac{\sin\chi \cos\delta \sin\beta \cos\epsilon}{\cos\left(\epsilon - \delta - \alpha_1\right)} \\ w &= \frac{\sin\delta \sin\beta \cos\epsilon}{\cos\left(\epsilon - \delta - \alpha_1\right)} \end{aligned}\right\} \tag{B15}$$

The entropy change across the shock is calculated from (ref. 22) as

$$\Delta s = s - s_\infty = \frac{1}{\gamma(\gamma - 1)} \ln\left[\frac{2\gamma}{\gamma + 1}\left(M_\infty{}^2 \sin^2\beta \sin^2\epsilon - \frac{\gamma - 1}{\gamma + 1}\right)\right] - \frac{1}{\gamma - 1} \ln\left[\frac{(\gamma + 1)M_\infty{}^2 \sin^2\beta \sin^2\epsilon}{2 + (\gamma - 1)M_\infty{}^2 \sin^2\beta \sin^2\epsilon}\right] \tag{B16}$$

APPENDIX C

CHARACTERISTIC AND COMPATIBILITY EQUATIONS

Any conical surface may be expressed as a function of the two coordinates ξ and η:

$$g(\xi,\eta) = \text{Constant}$$

$$dg = g_\xi \, d\xi + g_\eta \, d\eta = 0$$

The unit normal to the surface is

$$\hat{n} = \frac{\nabla g}{|\nabla g|}$$

Maslen (ref. 15) shows that the cross-flow velocity component – that is, the component normal to a ray from the apex – governs the type of partial differential equations in conical flow. For supersonic cross flow he shows that the characteristic surfaces are

$$U \cdot \hat{n} = a \qquad \text{and} \qquad U \cdot \hat{n} = 0$$

where $U \cdot \hat{n}$ can be expressed as

$$U \cdot \hat{n} = \frac{(\eta u - v)\frac{d\xi}{d\eta} - (\xi u - w)}{\sqrt{\left(\xi \frac{d\xi}{d\eta} - \eta\right)^2 + \left(\frac{d\xi}{d\eta}\right)^2 + 1}} \tag{C1}$$

For the case where $U \cdot \hat{n} = 0$ the characteristic surface is given by

$$\frac{d\xi}{d\eta} = \frac{\xi u - w}{\eta u - v} \tag{C2}$$

which is a surface consisting of streamlines.

From equation (6d) in the body of the paper, the compatibility relation is

$$ds = 0 \tag{C3}$$

This, of course, expresses the constancy of entropy along streamlines. The characteristic (C2) is a double characteristic since multiplying equation (6b) by $\eta u - v$ and equation (6c) by $\xi u - w$ and adding them gives

$$(\eta u - v)\left(u_\eta + \eta v_\eta + \xi w_\eta\right) + (\xi u - w)\left(u_\xi + \eta v_\xi + \xi w_\xi\right) = 0 \tag{C4}$$

It is found by inspection that equation (C2) defines a characteristic for equation (C4) for which the following compatibility relation applies:

$$du + \eta\, dv + \xi\, dw = 0 \tag{C5}$$

The equation $U \cdot \hat{n} = a$ is quadratic, and the two roots yield the slopes of two characteristics, one above and one below the stream surface:

$$\left(\frac{d\xi}{d\eta}\right)_\pm = \frac{a_1 \pm \sqrt{a_1^2 - a_1 a_3}}{a_2} \tag{C6}$$

These are the projections of the Mach cones in the cross-flow direction.

The remaining compatibility relations are found as follows. Equation (6d) and $ds = s_\eta\, d\eta + s_\xi\, d\xi$ yield the partial derivatives of s in terms of total differentials:

$$\left.\begin{aligned} s_\xi &= \frac{ds}{d\xi - \zeta\, d\eta} \\ s_\eta &= -\frac{\zeta\, ds}{d\xi - \zeta\, d\eta} \end{aligned}\right\} \tag{C7}$$

where

$$\zeta = \frac{\xi u - w}{\eta u - v} \tag{C8}$$

Multiplying equation (C4) by $d\eta$ and then adding and substracting the quantity $\left(u_\xi + \eta v_\xi + \xi w_\xi\right) d\xi$ yields

$$\left.\begin{aligned} u_\xi + \eta v_\xi + \xi w_\xi &= F_1 \\ u_\eta + \eta v_\eta + \xi w_\eta &= F_2 \end{aligned}\right\} \tag{C9}$$

where

$$\left.\begin{aligned} F_1 &= \frac{P}{d\xi - \zeta\, d\eta} \\ F_2 &= -\frac{\zeta P}{d\xi - \zeta\, d\eta} \\ P &= du + \eta\, dv + \xi\, dw \end{aligned}\right\} \tag{C10}$$

Substituting equations (C9) into either equation (6b) or equation (6c) yields

$$v_\xi - w_\eta = Q \tag{C11}$$

where

$$Q = \frac{a^2 ds + uP}{(\eta u - v)(d\xi - \zeta\, d\eta)} \tag{C12}$$

The continuity equation (7) may be written in the form

$$a^2 \xi u_\xi + a^2 \eta u_\eta + (\eta u - v)(\xi u - w)v_\xi - \left[a^2 - (\eta u - v)^2\right] v_\eta$$
$$- \left[a^2 - (\xi u - w)^2\right] w_\xi + (\eta u - v)(\xi u - w) = 0$$

or

$$a_1 v_\xi + a_2 v_\eta + a_3 w_\xi + a_1 w_\eta = G \tag{C13}$$

where

$$\left.\begin{aligned} G &= -a^2\left(\xi F_1 + \eta F_2\right) \\ a_1 &= a^2 \xi\eta - (\eta u - v)(\xi u - w) \\ a_2 &= a^2\left(1 + \eta^2\right) - (\eta u - v)^2 \\ a_3 &= a^2\left(1 + \xi^2\right) - (\xi u - w)^2 \end{aligned}\right\} \tag{C14}$$

Since

$$\left.\begin{aligned} v_\xi\, d\xi + v_\eta\, d\eta &= dv \\ w_\xi\, d\xi + w_\eta\, d\eta &= dw \end{aligned}\right\} \tag{C15}$$

equations (C15), equation (C11), and equation (C13) can be written in matrix form as

$$Ax = B \tag{C16}$$

where

$$A = \begin{vmatrix} a_1 & a_2 & a_3 & a_1 \\ 1 & 0 & 0 & -1 \\ d\xi & d\eta & 0 & 0 \\ 0 & 0 & d\xi & d\eta \end{vmatrix} \qquad x = \begin{vmatrix} v_\xi \\ v_\eta \\ w_\xi \\ w_\eta \end{vmatrix} \qquad B = \begin{vmatrix} G \\ Q \\ dv \\ dw \end{vmatrix} \tag{C17}$$

The determinant of the coefficient matrix A is

$$|A| = a_2\, d\xi^2 - 2a_1\, d\xi\, d\eta + a_3\, d\eta^2 \tag{C18}$$

When the determinant vanishes, it gives the slope of the characteristics, equation (C6). To find the compatibility equations, the determinant

$$\begin{vmatrix} a_1 & a_2 & a_3 & G \\ 1 & 0 & 0 & Q \\ d\xi & d\eta & 0 & dv \\ 0 & 0 & d\xi & dw \end{vmatrix}$$

is equated to zero, or

$$G - a_1 Q + \frac{d\xi}{d\eta} a_2 Q - a_2 \frac{dv}{d\eta} - a_3 \frac{dw}{d\xi} = 0 \tag{C19}$$

Substituting values of G and Q gives

$$b_1\, du + b_2\, dv + b_3\, dw + b_4\, ds = 0 \tag{C20}$$

where

$$\left.\begin{aligned} b_1 &= -a^2(\xi v - \eta w) - \left(a_1 - a_2 \frac{d\xi}{d\eta}\right) u \\ b_2 &= a_2\left[(\xi u - w) - (\eta u - v)\frac{d\xi}{d\eta}\right] - a^2\eta(\xi v - \eta w) - \eta u\left(a_1 - a_2 \frac{d\xi}{d\eta}\right) \\ b_3 &= -a^2\xi(\xi v - \eta w) - \xi u\left(a_1 - a_2 \frac{d\xi}{d\eta}\right) + \frac{a_3 a_2\left[(\xi u - w) - (\eta u - v)\frac{d\xi}{d\eta}\right]}{a_2 \frac{d\xi}{d\eta}} \\ b_4 &= -a^2\left(a_1 - a_2 \frac{d\xi}{d\eta}\right) \end{aligned}\right\} \tag{C21}$$

Equation (C20) is the compatibility equation, which is the condition to be fulfilled along any characteristic given by equation (C6).

REFERENCES

1. Browne, S. H.; Friedman, L.; and Hodes, I.: A Wing-Body Problem in a Supersonic Conical Flow. J. Aeronaut. Sci., vol. 15, no. 8, Aug. 1948, pp. 443-452.

2. Goldstein, S.; and Ward, G. N.: The Linearised Theory of Conical Fields in Supersonic Flow, With Applications to Plane Aerofoils. Aeronaut. Quart., vol. II, pt. I, May 1950, pp. 39-84.

3. Lagerstrom, P. A.: Linearized Supersonic Theory of Conical Wings (Corrected copy). NACA TN 1685, 1950.

4. Babaev, D. A.: Numerical Solution of the Problem of Supersonic Flow Past the Lower Surface of a Delta Wing. AIAA J., vol. 1, no. 9, Sept. 1963, pp. 2224-2231.

5. Babayev, D. A.: Numerical Solution of the Problem of Flow Round the Upper Surface of a Triangular Wing by a Supersonic Stream. U.S.S.R. Comput. Math. Math. Phys. no. 2, 1963, pp. 296-308.

6. Bulakh, B. M.: On the Theory of Nonlinear Conical Flows. Appl. Math. Mech. (Moscow), vol. 19, no. 4, 1955, pp. 393-409. (Also available in English translation as TR-16, Grumman Aircraft Eng. Corp., 1955.)

7. Bulakh, B. M.: Remarks on the Paper by L. R. Fowell, "Exact and Approximate Solutions for the Supersonic Delta Wing." J. Appl. Math. Mech., vol. 22, no. 3, 1958, pp. 562-567.

8. Bulakh, B. M.: Some Questions Concerning the Theory of Conical Flow. J. Appl. Math. Mech., vol. 25, no. 2, 1961, pp. 339-356.

9. Bulakh, B. M.; and Reyn, J. W.: Remarks on the Problem of the Delta-Shaped Wing. J. Appl. Math. Mech., vol. 31, no. 1, 1967, pp. 207-210.

10. Bulakh, B. M.: Comments on the paper by A. Ferri, "Recent Theoretical Work in Supersonic Aerodynamics at the Polytechnic Institute of Brooklyn." J. Appl. Math. Mech., vol. 23, no. 3, 1959, pp. 811-818.

11. Busemann, Adolf: Infinitesimal Conical Supersonic Flow. NACA TM 1100, 1947.

12. Ferri, Antonio; Vaglio-Laurin, Roberto; and Ness, Nathan: Mixed Type Conical Flow Without Axial Symmetry – Summary of the Recent Work Performed at P.I.B.A.L. PIBAL Rep. No. 264 (Contract No. AF 18(600)-186), Polytech. Inst. Brooklyn, Dec. 1954.

13. Fowell, L. R.: Exact and Approximate Solutions for the Supersonic Delta Wing. J. Aeronaut. Sci., vol. 23, no. 8, Aug. 1956, pp. 709-720, 770.

14. Bazzhin, A. P.; Trusova, O. N.; and Chelysheva, I. F.: Calculation of Ideal-Gas Flows Around Elliptical Cones at Large Angles of Attack. Izv. Akad. Nauk SSSR, Mekh. Zhidk. Gaza, no. 4, 1968, pp. 45-51.

15. Maslen, Stephen H.: Supersonic Conical Flow. NACA TN 2651, 1952.

16. Goldstein, Sydney: Lectures on Fluid Mechanics. Vol. II of Lectures in Applied Mathematics, Interscience Publishers, c.1960.

17. Vincenti, Walter G.; and Fisher, Newman H., Jr.: Calculation of the Supersonic Pressure Distribution on a Single-Curved Tapered Wing in Regions Not Influenced by the Root or Tip. NACA TN 3499, 1955.

18. Love, E. S.: Generalized-Newtonian Theory. J. Aero/Space Sci. (Readers' Forum), vol. 26, no. 5, May 1959, pp. 314-315.

19. Wagner, Richard D., Jr.; and Watson, Ralph: Reynolds Number Effects on the Induced Pressures of Cylindrical Bodies With Different Nose Shapes and Nose Drag Coefficients in Helium at a Mach Number of 24. NASA TR R-182, 1963.

20. Bertram, Mitchel H.: An Approximate Method for Determining the Displacement Effects and Viscous Drag of Laminar Boundary Layers in Two-Dimensional Hypersonic Flow. NACA TN 2773, 1952.

21. South, Jerry C., Jr.; and Klunker, E. B.: Methods for Calculating Nonlinear Conical Flows. Analytic Methods in Aircraft Aerodynamics, NASA SP-228, 1970, pp. 131-155; Discussion, pp. 156-158.

22. Ames Research Staff: Equations, Tables, and Charts for Compressible Flow. NACA Rep. 1135, 1953. (Supersedes NACA TN 1428.)

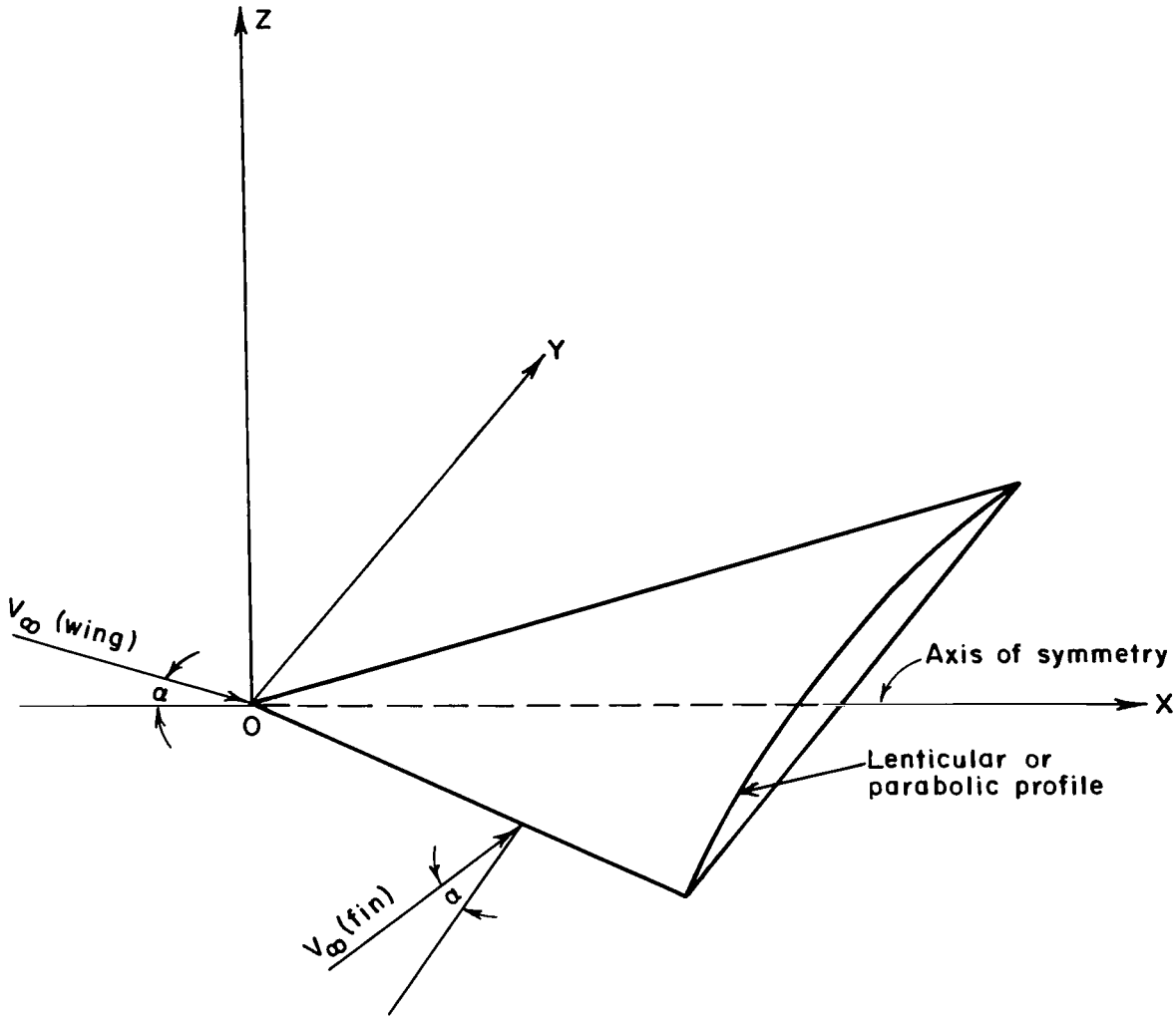

Figure 1.- Configuration of a fin or a wing.

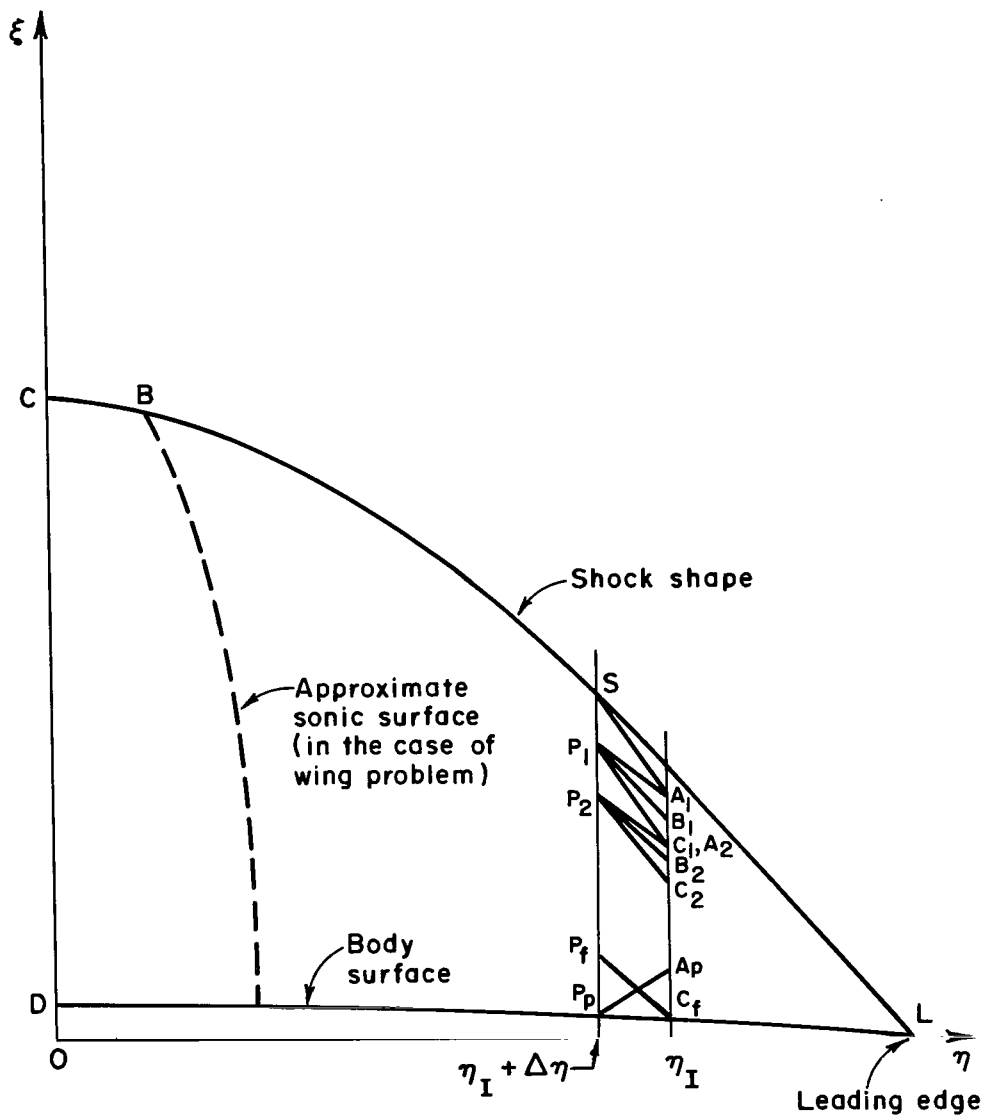

Figure 2.- Sketch showing computing technique.

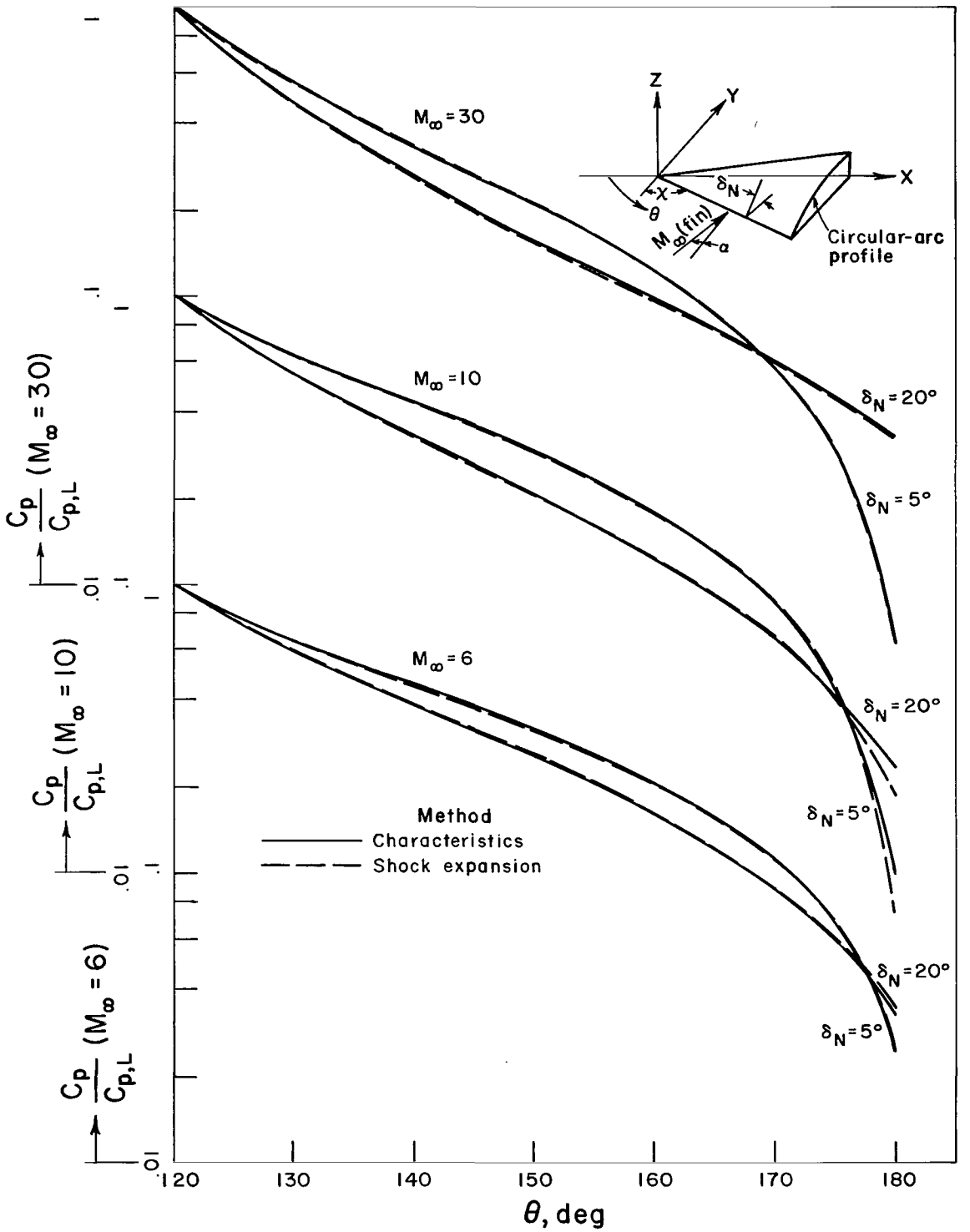

Figure 3.- Accelerating cross flows over circular-arc fin. $\chi = 30^0$; $\gamma = 1.400$; $\alpha = 0^0$.

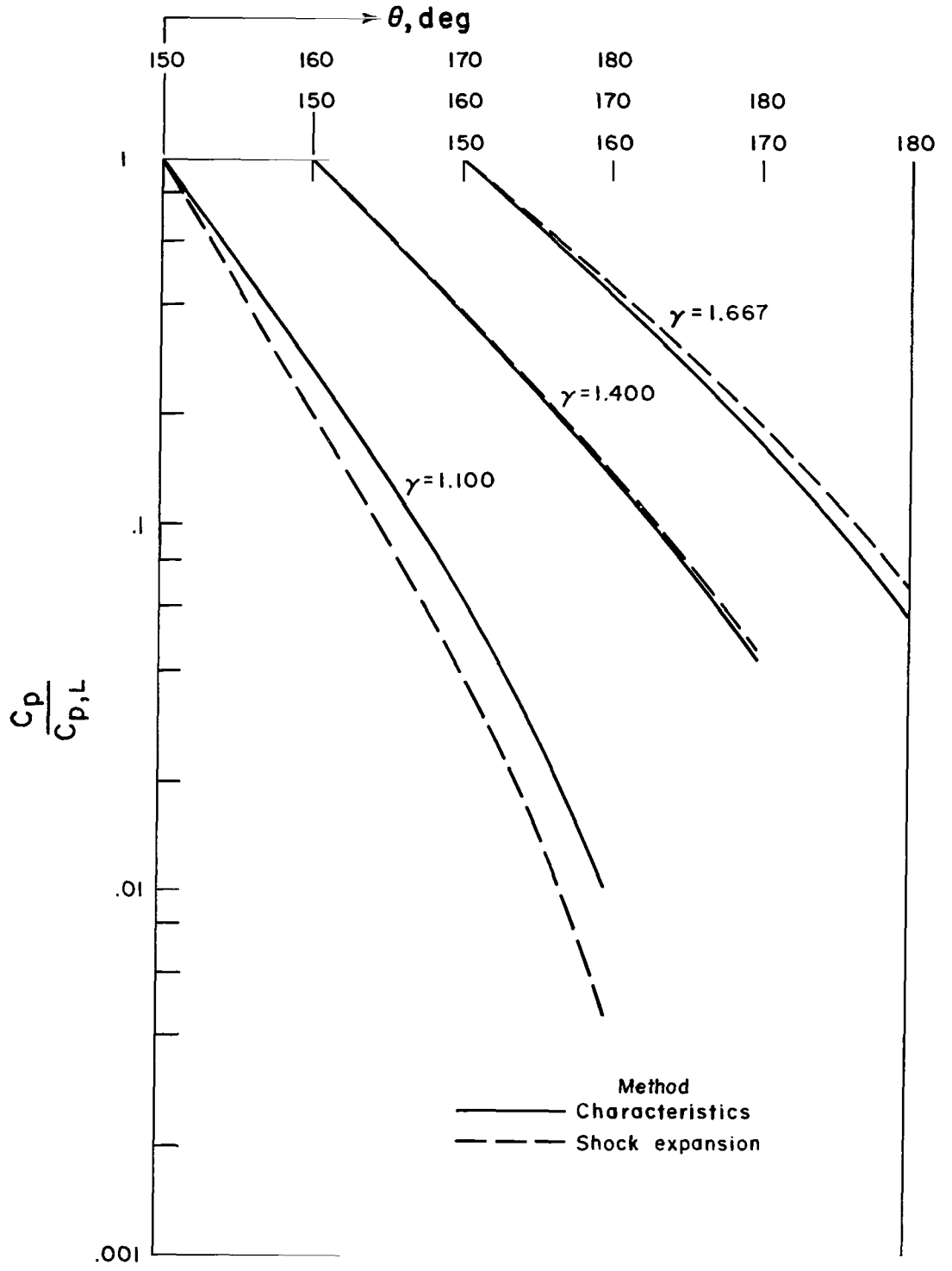

Figure 4.- Effect of γ for circular-arc fins. $M_\infty = 30$; $\delta_N = 30^0$; $\chi = 60^0$; $\alpha = 0^0$.

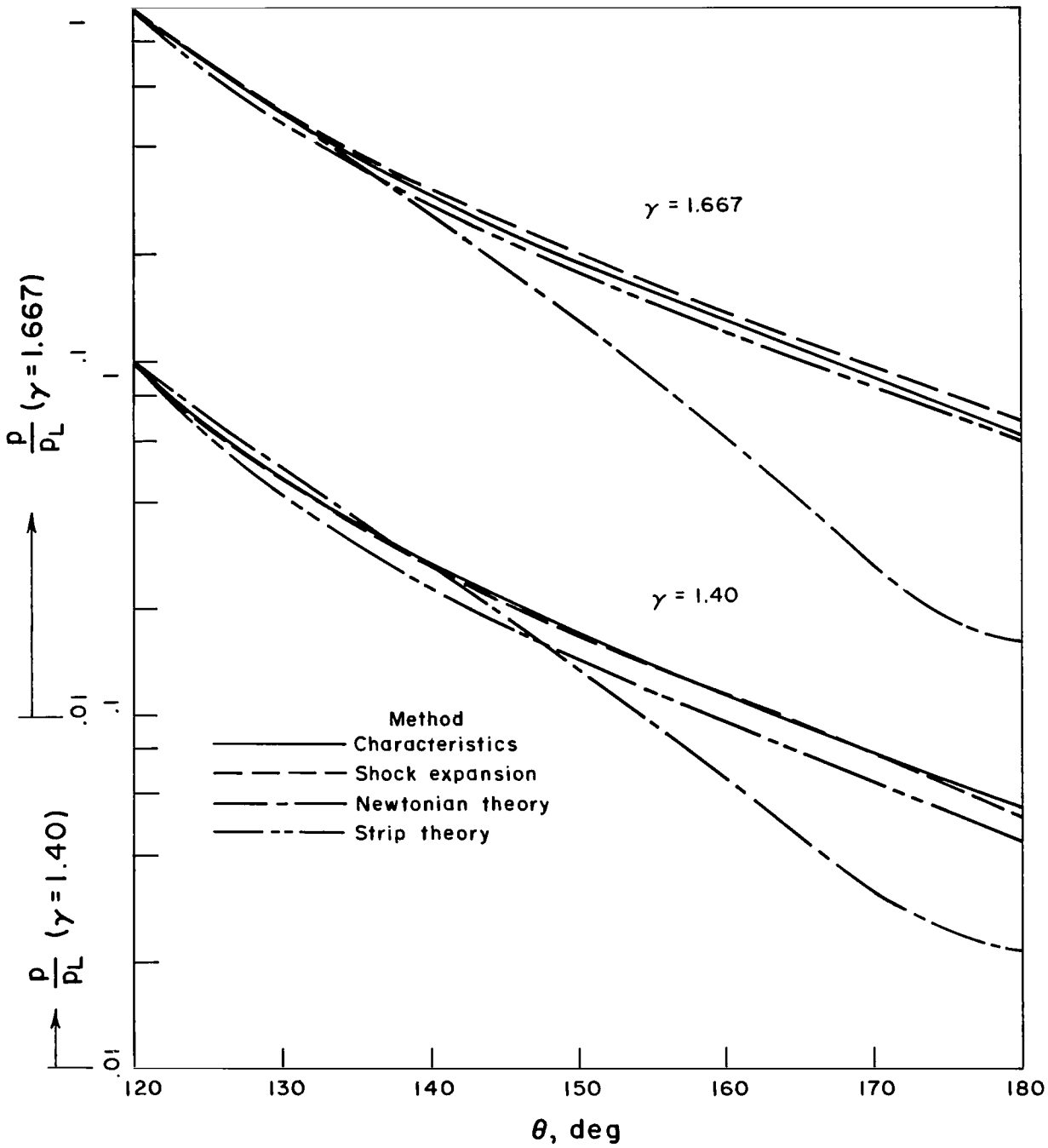

Figure 5.- Comparisons between various theories for circular-arc fins. $\alpha = 0^0$; $\chi = 30^0$; $\delta_N = 20^0$; $M_\infty = 30$.

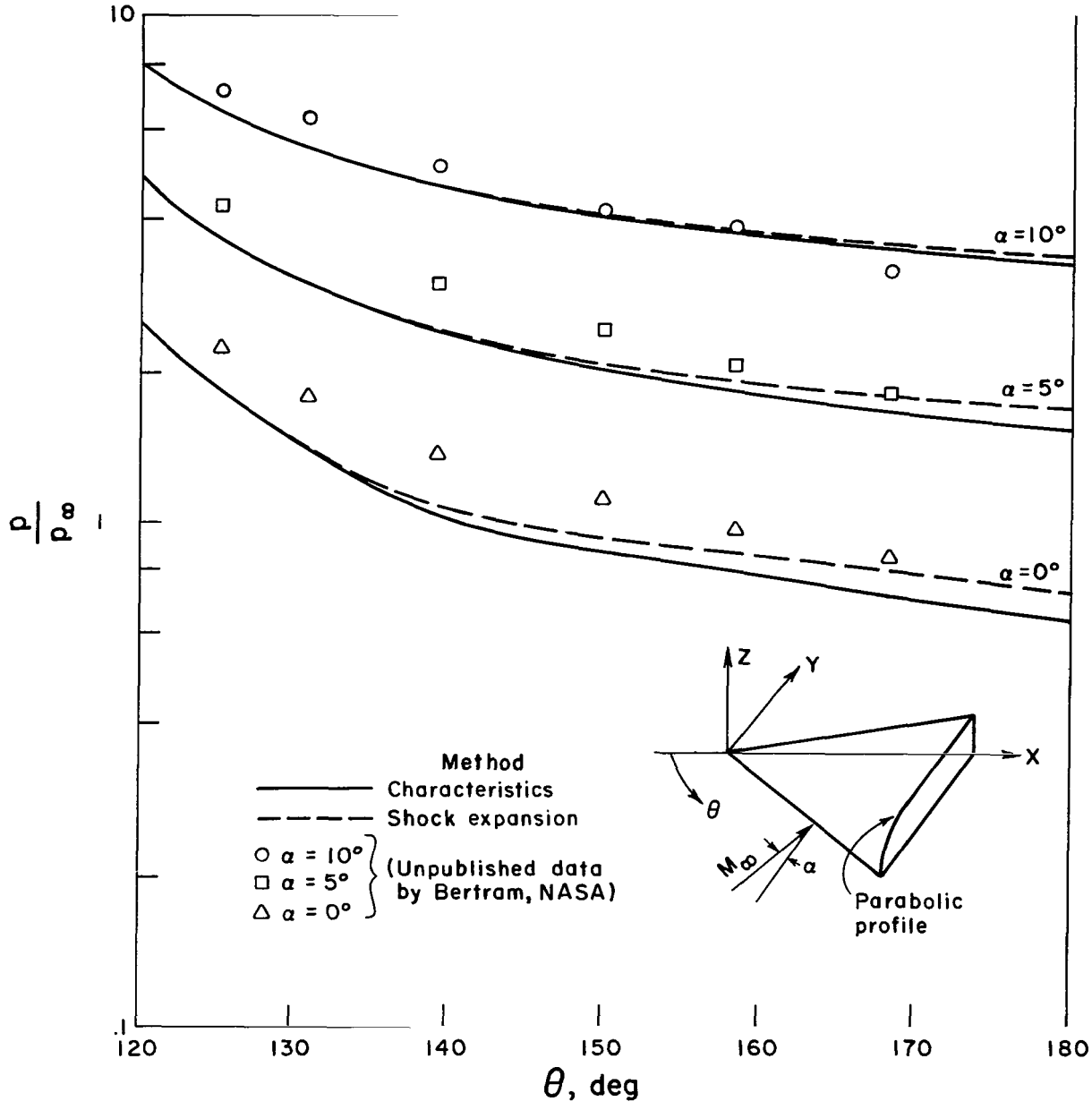

Figure 6.- Comparison of theoretical and experimental results for parabolic fin. $\chi = 30^0$; $M_\infty = 6.85$; $\gamma = 1.40$.

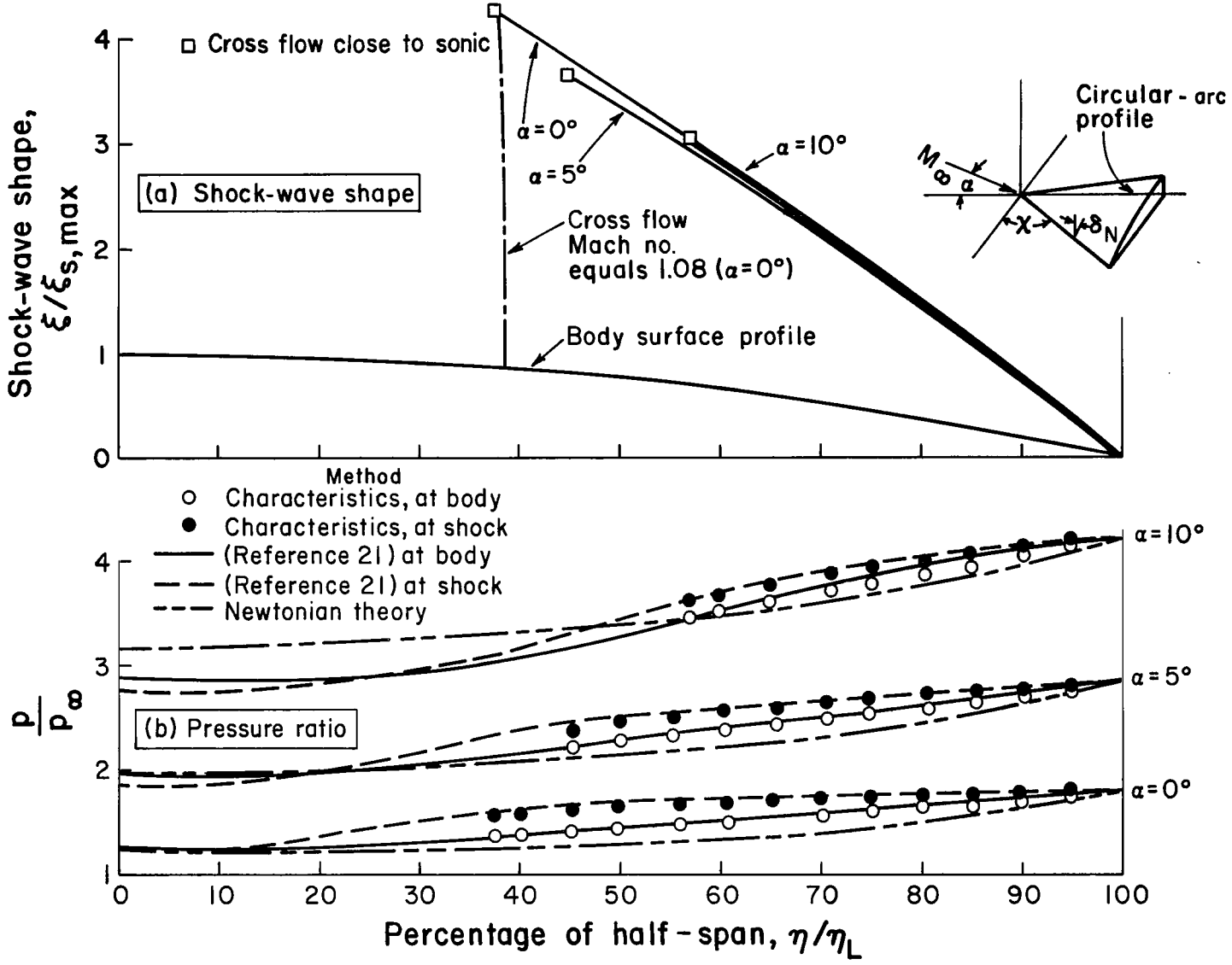

Figure 7.- Shock-wave shape and pressure ratio as a function of percentage of half-span for a circular-arc wing. $\gamma = 1.40$; $M_\infty = 4.0$; $\delta_N = 9^0 18'$; $\chi = 50^0$.

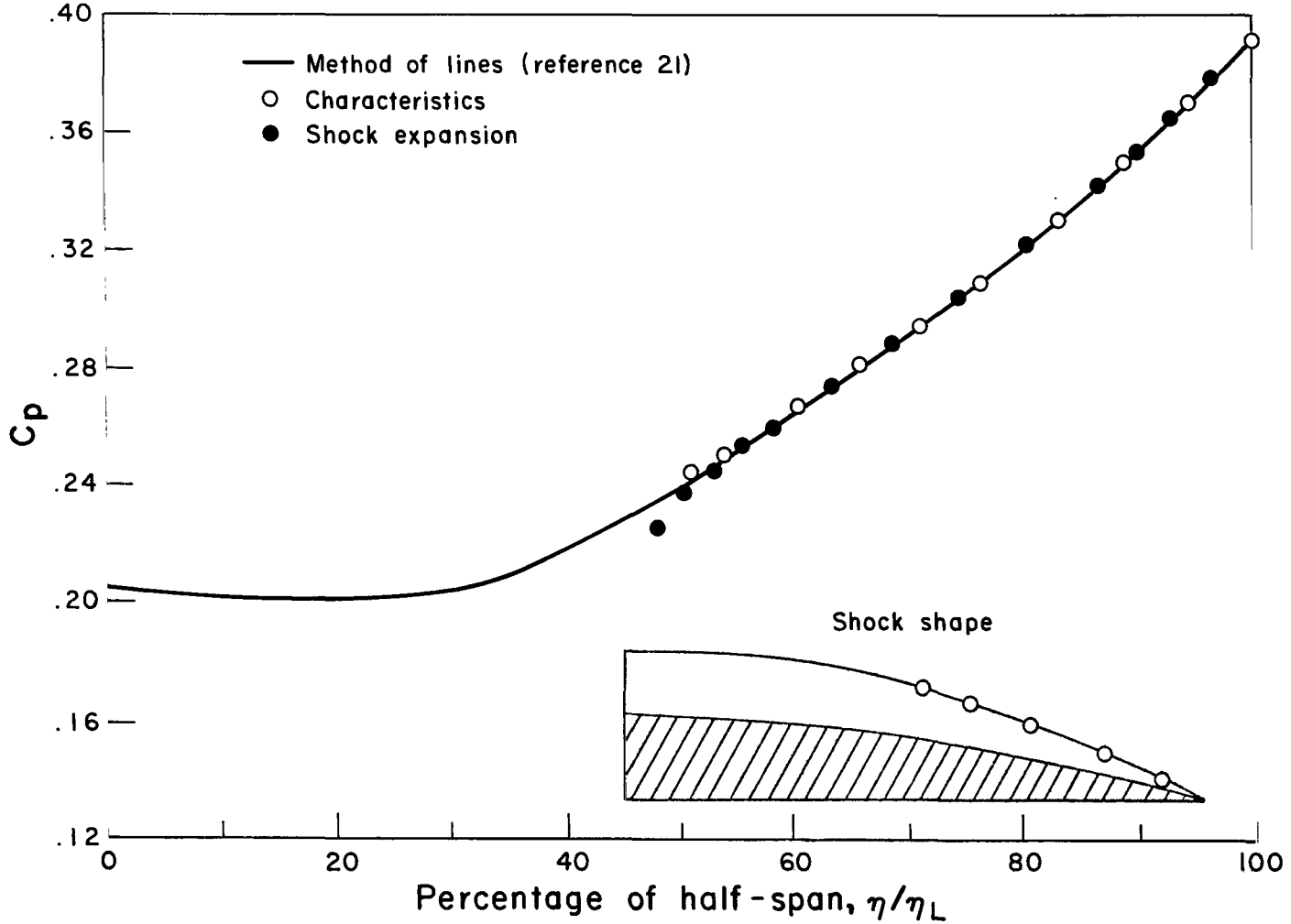

Figure 8.- Pressure coefficient C_p as a function of percentage of half-span for a circular-arc wing. $M_\infty = 8.1$; $\chi = 50^0$; $\alpha = 10^0$; $\delta_N = 20^0$.

NATIONAL AERONAUTICS AND SPACE ADMINISTRATION
WASHINGTON, D.C. 20546
OFFICIAL BUSINESS

FIRST CLASS MAIL

POSTAGE AND FEES PAID
NATIONAL AERONAUTICS AND
SPACE ADMINISTRATION

07U 001 37 51 3DS 70185 00903
AIR FORCE WEAPONS LABORATORY /WLOL/
KIRTLAND AFB, NEW MEXICO 87117

ATT E. LOU BOWMAN, CHIEF, TECH. LIBRARY

....STER: If Undeliverable (Section 158 Postal Manual) Do Not Return

"The aeronautical and space activities of the United States shall be conducted so as to contribute . . . to the expansion of human knowledge of phenomena in the atmosphere and space. The Administration shall provide for the widest practicable and appropriate dissemination of information concerning its activities and the results thereof."

—NATIONAL AERONAUTICS AND SPACE ACT OF 1958

NASA SCIENTIFIC AND TECHNICAL PUBLICATIONS

TECHNICAL REPORTS: Scientific and technical information considered important, complete, and a lasting contribution to existing knowledge.

TECHNICAL NOTES: Information less broad in scope but nevertheless of importance as a contribution to existing knowledge.

TECHNICAL MEMORANDUMS: Information receiving limited distribution because of preliminary data, security classification, or other reasons.

CONTRACTOR REPORTS: Scientific and technical information generated under a NASA contract or grant and considered an important contribution to existing knowledge.

TECHNICAL TRANSLATIONS: Information published in a foreign language considered to merit NASA distribution in English.

SPECIAL PUBLICATIONS: Information derived from or of value to NASA activities. Publications include conference proceedings, monographs, data compilations, handbooks, sourcebooks, and special bibliographies.

TECHNOLOGY UTILIZATION PUBLICATIONS: Information on technology used by NASA that may be of particular interest in commercial and other non-aerospace applications. Publications include Tech Briefs, Technology Utilization Reports and Notes, and Technology Surveys.

Details on the availability of these publications may be obtained from:

SCIENTIFIC AND TECHNICAL INFORMATION DIVISION

NATIONAL AERONAUTICS AND SPACE ADMINISTRATION

Washington, D.C. 20546